THE RELATION BETWEEN POLYHEDRAL BORANE SANDWICHES AND ENDOHEDRAL COMPLEXES; THE ELECTRONIC STRUCTURE AND STABILITY OF $X@Y_mB_nH_{n+m}^q$ (X = He, Ne, Li, Be; Y = B, C, Si; m = 0–3; n = 12–9; q = –2 to +2), $(C_2B_4H_6)_2X^q$ (X = Li, Al, Si; q = –3, –1, 0) AND $X_2@B_{17}H_{17}^q$ (X = He, Li; q = –2, 0)

Eluvathingal D. JEMMIS[1,*] and Elambalassery G. JAYASREE[2]

School of Chemistry, University of Hyderabad, Hyderabad-500046, India;
e-mail: [1] jemmis@uohyd.ernet.in, [2] edjscrs@uohyd.ernet.in

Received April 8, 2002
Accepted May 14, 2002

This paper is dedicated to Professor Jaromír Plešek on the occasion of his 75th birthday.

An electronic structural connection is established for sandwich complexes and polyhedral boranes containing encapsulated atoms. The charge requirements of these extreme geometrical patterns, examples **3** and **9**, depend on the size of the central atom or on the distance between the adjacent rings. While going from the endohedral to the corresponding sandwich complexes the unoccupied a_{2u} and e_g molecular orbitals are stabilized considerably requiring additional 6 electrons for stability. The two endohedral atoms in the doped structures **10** resulting from the multidecker sandwich complexes **4** are found to stabilize the large borane skeleton. The energetics and geometries of the relatively less explored endohedral boranes show that endohedral silaboranes are more stable than the endohedral carbaboranes. In general, when an atom is encapsulated in a borane cage, its skeletal bonds are elongated. The exo bonds are shortened due to the possible reduction in the torsional strain between the adjacent vertices. A comparison of the endohedral complexes with the corresponding exo isomers shows that encapsulation makes the system more strained.
Keywords: Sandwich complexes; Polyhedral boranes; Metallaboranes; Carboranes; Endohedral complexes; *Ab initio* calculations.

Sandwich complexes occupy a prominent place in chemistry. Though a large majority of these are known with Cp^- ($C_5H_5^-$) (**1**) and similar planar rings[1], there are several examples known with polyhedral borane fragments such as the pentagonal pyramidal $C_2B_4H_6^{2-}$ (**2**, **3**)[2–7], the ollide ions $C_2B_9H_{11}^{2-}$ [8–10] and the $B_{11}H_{11}^{4-}$ (**5**, **7**)[11] as ligands. Recognition of the similarity between the frontier orbitals of Cp^- and of the polyhedral fragments $C_2B_9H_{11}^{2-}$ and $C_2B_6H_6^{2-}$ was a turning point in this chemistry[12]. The struc-

tural connection between a sandwich complex involving two pentagonal pyramids (**3**) and an icosahedron generated by bringing them closer (**9**) cannot be missed. If the sandwiched central atom is not retained, the traditional monocage polyhedral borane results. The icosahedral structure with a central atom belongs to the family of endohedral complexes, which have been studied rigorously during recent years[13]. These are known experimentally with the fullerenes[13a–13d] and even with the classic strained hydrocarbon, $C_{20}H_{20}$ with icosahedral symmetry[13e]. To our knowledge, no endohedral complex of polyhedral borane is reported experimentally even though recent theoretical studies have shown that several of them are minima on their potential energy surface[14]. In view of the many sandwich structures involving the polyhedral fragments with a main group atom at the centre, there is indeed the possibility of generating endohedral structures of the same kind. An encapsulated boron atom inside a polyhedral arrangement is observed in the structure of β-rhombohedral boron[15]. The related $B_{28}H_{18}^{+}$ (C_{3v}) is calculated to be a minimum[15c]. A point of concern is also that there is no known sandwich structure of the type **3** available with boron as the central atom. The only sandwich structure with a central boron atom calculated to be a minimum has $Si_3H_3^{+}$ as ligands[16].

We have studied the requirements for stabilizing sandwich and endohedral complexes involving the main-group atoms. A preliminary report on endohedral complexes was published previously[14a]. We had also developed an electron-counting rule that is applicable to sandwich complexes as well as endohedral structures[17]. However, details of the interaction that precludes **3** with a central boron atom are not known. A more general understanding, which examines the interrelationship between a variety of sandwich structures and the corresponding endohedral structures is needed. We attempt such an understanding by an analysis of the molecular orbitals, Walsh diagrams generated for the transformation of the sandwich complexes to the corresponding endohedral structures (Fig. 1) and quantitative studies on selected examples. Correlation diagrams that connect the pentagonal pyramidal fragments, their sandwich complexes with Si and B as the central atom and the corresponding endohedral complexes also help in this study. We also analyze structures with three pentagonal bipyramids (**4**) and complexes of ollide ions (**5**–**7**) in place of pentagonal pyramids, and their corresponding endohedral isomers (**10**, **11**–**13**). The dependence of the stability of the endohedral boranes on the size of the parent cage as well as the size of the central atom are examined using the mono, di- and trisubstituted twelve-vertex carbaboranes and silaboranes varying the central atom (Fig. 2). A comparison of the relative energies of the stuffed sys-

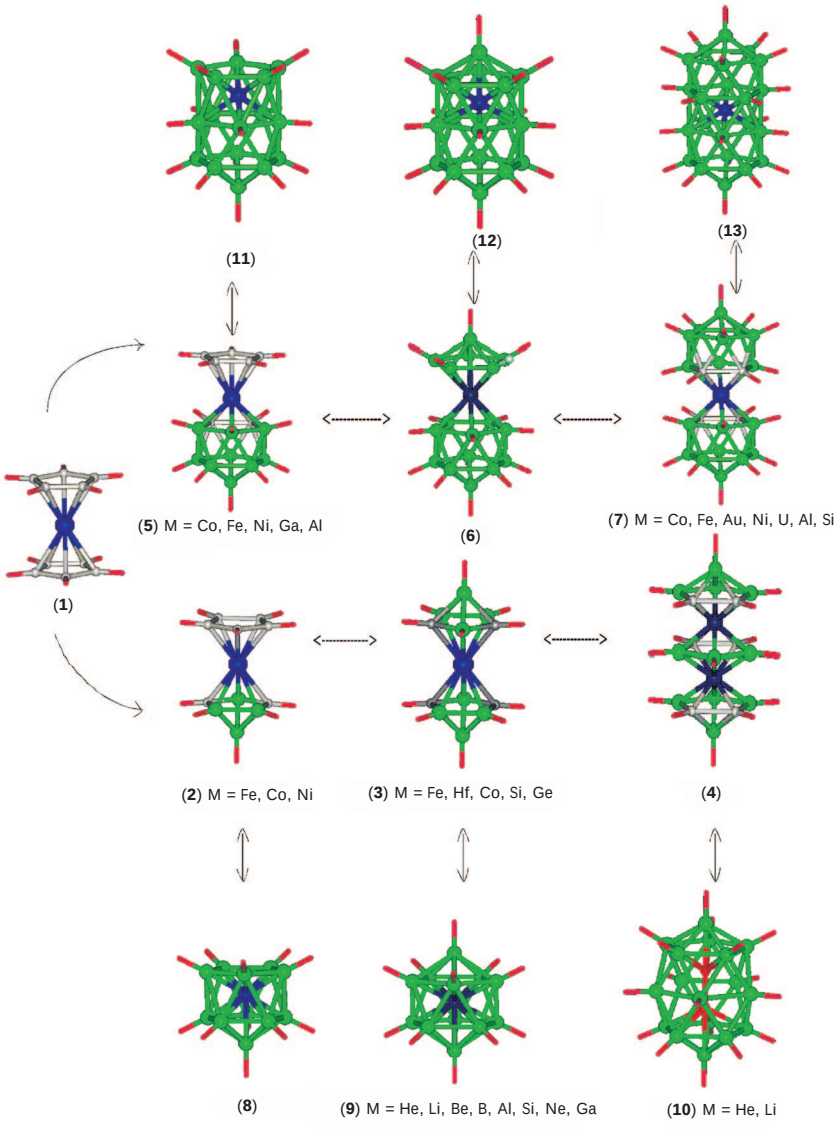

FIG. 1

The continuum of structures generated from sandwich structures similar to ferrocene and the corresponding endohedral structures. The central atoms of experimentally characterized or theoretically favorable structures are mentioned below each category. Charges of the respective molecules are not given due to the variety in the metal centers

tems with respect to the corresponding exo isomer in which the heteroatom caps a face of the polyhedron helps to calibrate the stabilities of various endohedral complexes. Near-isodesmic equations are used to obtain relative preferences in a given series of endohedral complexes.

COMPUTATIONAL METHODOLOGY

A qualitative molecular orbital analysis is carried out for the single vertex sharing systems and the corresponding endohedral compounds using extended Hückel theory[18]. Quantitative studies of the sandwich and endohedral complexes discussed in the paper are carried out at the B3LYP/6-31G* [19] level of theory using the Gaussian94 programme[20]. The vibrational frequencies for all the structures are computed at the same level of theory. In general the complexes are numbered as **N(a–g)-X**$_n$ where **N** corresponds to the number of structure shown in Fig. 1, **X** corresponds to the central atom, **a**–**g** correspond to the parent cages (**a**) $B_{12}H_{12}^{2-}$, (**b**) $CB_{11}H_{12}^{-}$, (**c**) $C_2B_{10}H_{12}$, (**d**) $C_3B_9H_{12}^{+}$, (**e**) $SiB_{11}H_{12}^{-}$, (**f**) $Si_2B_{10}H_{12}$, and (**g**) $Si_3B_9H_{12}^{+}$ in endohedral complexes. The exohedral isomers are differentiated from the endohedral ones by a prime added at the end of the label. The positional isomers para, meta and ortho of dicarbaborane are identified by the

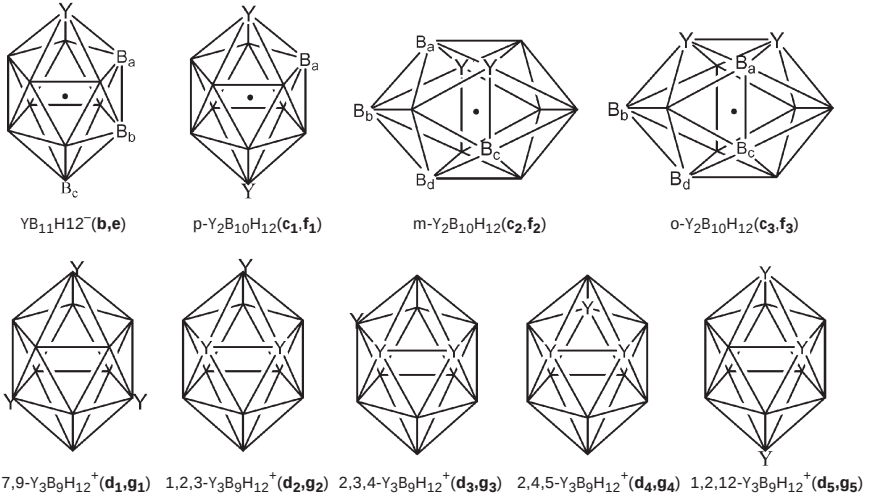

FIG. 2

The parent cages along with the vertex symbols used in the text, Y = C, Si. Symbols given in parentheses are: **b** for monocarbaborane cage, **c** for dicarbaboranes and **d** for tricarbaboranes. Similarly **e**, **f** and **g** represent the mono-, di- and trisilaboranes

subscripts 1, 2 and 3, respectively, and those of tricarbaboranes are given numbers 1 to 5 as shown in Fig. 2. Thus, **9a-Li** corresponds to the endohedral complex represented by **9** with the icosahedral $B_{12}H_{12}^{2-}$ skeleton (**a**) with Li^+ inside ($Li@B_{12}H_{12}^-$) and **10a-Li$_2$** stands for $Li_2@B_{17}H_{17}$. The total energies, relative energies, zero-point energies and the HOMO-LUMO gap of each compound are given in Tables I and II. The energy of encapsulation and that of capping is included in Table III. The stability order of the structures based on the values obtained using the near-isodesmic equations (Table IV) provides further comparison. Important geometrical parameters discussed in the paper are given in Tables V and VI.

RESULTS AND DISCUSSION

We present a discussion of the electronic requirements of the various structures involved based on qualitative Walsh diagrams and correlation diagrams, mostly based on extended Huckel calculations. This is followed by an analysis of geometries and the energetics of selected structures studied quantitatively. Comparison of the endohedral structures with competing and more favorable exohedral structures are made at the end.

Qualitative Analysis of the Electronic Structure of Endohedral and Sandwich Complexes

We begin the analysis by constructing a correlation diagram that connects pentagonal pyramidal B_6H_6 fragments, sandwiches of the type **3** (M = Si, B), endohedral complexes **9** (M = B) and $B_{12}H_{12}^{2-}$ (Fig. 3). While going from a hypothetical polyhedron made of two pentagonal pyramids with large ring–ring distance (Fig. 3, **B**) to a sandwich structure with a large central atom such as silicon (Fig. 3, **C**), the a_{2u} orbital is significantly stabilized by the favorable interaction with the suitable orbital of the central atom. Many structures of this type are known experimentally[2–7]. Bridging the two pentagonal pyramids by an atom smaller than silicon, for example, boron (Fig. 3, **D**), increases the direct unfavorable interactions between the two. Hence a_{2u} and e_g orbitals are pushed up in energy leading to a decreased electronic requirement for the structure. This is in tune with the nonexistence of the sandwich complexes of pure polyhedral boranes. When the rings flanking the central atom are brought closer so that an encapsulated arrangement results, the a_{2u} molecular orbital goes up in energy even more dramatically (Fig. 3, **E**). The molecular orbital pattern emerging from this correlation is similar to that of the parent polyhedron without a central

atom. Thus, the electronic requirements of the polyhedron do not change by encapsulation. The charge of the endohedral system will differ from the parent cage, reflecting the contribution of the valence electrons of the central atom for skeletal bonding. Hence $B@B_{12}H_{12}$ should have a charge of +1 to compensate the three electrons contributed by the central boron atom to the $B_{12}H_{12}^{2-}$.

The newly established *mno* rule for polyhedral boranes, which is an extension of Wade's rule, explains the HOMO-LUMO separations found for various structures in Fig. 3 [17]. According to this rule, $m + n + o$ skeletal pairs are required for the stability of any polyhedral borane. Here m is the number of cages, n is the total number of vertices and o is the number of single-vertex-sharing linkages between clusters. Any electron-counting rule has to be used with caution. These represent the electronic requirements at the extremes. Often chemistry offers a continuum of examples. We have studied

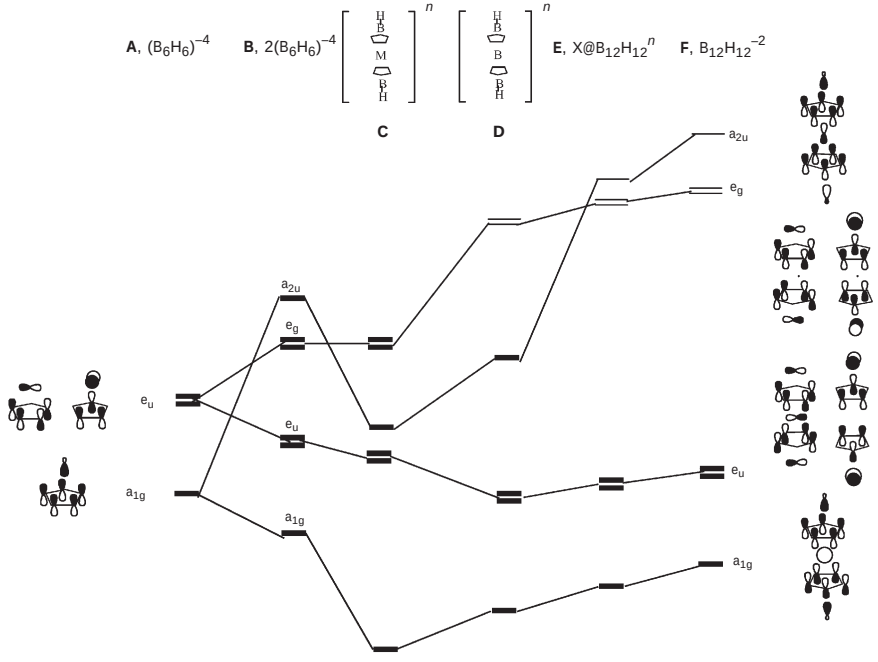

FIG. 3

Correlation diagram connecting two $B_6H_6^{4-}$ fragments (**A**, **B**), sandwich structures with central atom boron and silicon (**C**, **D**), and the endohedral polyhedron (**E**). **F** represents the MOs of parent polyhedron, $B_{12}H_{12}^{2-}$. The MOs shown on the right side are those of single-atom-bridged structures

the Walsh diagram connecting the sandwich complex to the corresponding encapsulated polyhedron as a function of ring–ring distance (Fig. 4). The stabilization of $1a_{2u}$ and $2e_g$ orbitals in going from the endohedral to the sandwich complex is clear from the diagram. At a ring–ring distance of around 2.6 Å or when the bridging atom is small, there is no marked HOMO-LUMO gap since $2e_u$, $1a_{2u}$, $2e_g$, and $3e_g$ are separated by small energies (Fig. 4) and it is difficult to differentiate the HOMO and LUMO from the Walsh diagram, which shows the variable electronic requirements for such structures. This point corresponds to the boron-bridging complexes shown in Fig. 3, **D**. A parallel analysis is carried out for the variation of electronic structure for **2**, **5**, **6**, and **7** going to their corresponding endohedral structures **8**, **11**, **12**, and **13**, respectively. Similar correlation diagrams are obtained with nearly identical electron requirement in other examples of Fig. 1. The HOMO-LUMO gap and the stabilization of one doubly degenerate and a non-degenerate MO for the sandwich structures are always ob-

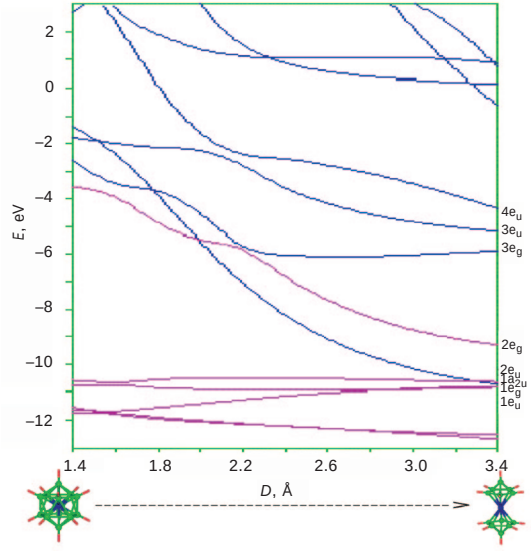

FIG. 4

The Walsh diagram connecting the encapsulated and single-vertex-sharing polyhedral $B_{13}H_{12}$ systems. The distance (*D*) between the two 5-membered rings is plotted along the *x*-axis. The energy (*E*) is plotted along the *y*-axis. e_u is the HOMO of the endohedral system and as the distance between the rings increases gradually, e_g and a_{2u} come down in energy, and e_g becomes the HOMO. The optimized structure of the endohedral $B@B_{12}H_{12}^+$ is shown

tained. Thus, in all the cases the sandwich structures require six electrons more than the endohedral structures. Obviously the *nido* systems (**2**, **5**) require 2 more electrons than the *closo*. Examples of complexes **2** [21], **3** [2–7], **5** [22], and **7** [8–10] are known in the literature.

The extension to one more cage will result in structures similar to that in transition metal cluster chemistry. The Walsh diagram for the structure $B_6H_6LiB_5H_5LiB_6H_6$ (**4-Li$_2$**) going to its endohedral analog $Li_2@B_{17}H_{17}$ (**10a-Li$_2$**) is shown in Fig. 5. The presence of two atoms inside the cage does not change the observed behavior as in the case of single atom encapsulated cages. The valence electrons of the stuffed atoms satisfy the electronic requirements for the skeletal framework of the polyhedron. As per the *mno* rule the structure **4-Li$_2$** requires 24 (3 + 19 + 2) electron pairs and the structure **10a-Li$_2$** requires 18 (1 + 17) electron pairs. The BH vertices provide 17 electron pairs and the 2 central lithium atoms together contribute one elec-

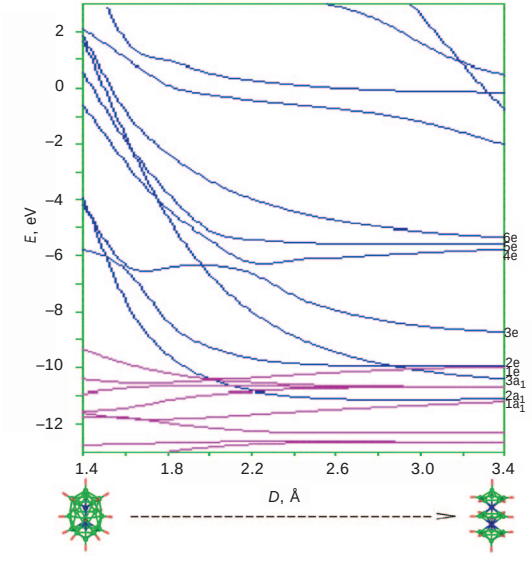

FIG. 5

The Walsh diagram connecting the three-cage single-vertex-sharing system $[B_6H_6LiB_5H_5LiB_6H_6]$ (**4-Li$_2$**) and its two atom encapsulated counterparts $Li_2@B_{17}H_{17}$ (**10a-Li$_2$**). The stabilization of two doubly degenerate MOs (LUMO (2e) and LUMO+1 (3e) of endohedral systems) and two non-degenerate MOs (LUMO+2 ($2a_1$) and another higher-lying antibonding orbital ($3a_1$)) in the sandwich structure shows that it requires 6 electron pairs more than the endohedral complex. The *x*-axis shows the distance (*D*) between the two adjacent rings and *y*-axis the energy (*E*). The optimized structure of $Li_2@B_{17}H_{17}$ is shown

tron pair in both the structural varieties. Thus, the structure **10a-Li$_2$** is neutral and the structure **4-Li$_2$** requires 6 more electron pairs. While going from **10a-Li$_2$** to **4-Li$_2$**, the stabilization of two doubly degenerate MOs (2e, 3e) and 2 non-degenerate MOs ($2a_1$, $3a_1$) is obvious from Fig. 5, which is in agreement with the *mno* rule. The electronic requirements anticipated by the above analysis are substantiated by the presence of experimentally characterized complexes *viz.* $[(R_2C_2B_4H_4)Co(C_2B_3H_5)]^-$ (**2**)[21]; $((SiMe_3)_2C_2B_4H_4)_2Si$, $[Li(C_2B_4H_5SiMe_3)_2]^-$, $[((SiMe_3)_2C_2B_4H_4)_2Ga]^-$ (**3**)[2–7]; $[(C_2B_9H_{11})MCp]$ [22] (where M = Fe, CO, Ni, Ga, Al) (**5**) and $[(C_2B_9H_{11})_2M]$ [8–10] (M = Fe, Co, Ni, Si, Al) (**7**).

The structures $[(C_2B_4H_6)_2Al]^-$ (**3-Al**), $(C_2B_4H_6)_2Si$ (**3-Si**), $[(C_2B_4H_6)_2Li]^{3-}$ (**3-Li**) are calculated to be minima on the potential energy surface (PES) with the lowest frequency 27.63, 4.08 and 21.10, respectively (Fig. 6). The lowest frequencies correspond to the rotation of the rings along the pseudo C_5 axis. However, similar sandwich complexes with comparatively smaller atoms as the sharing vertex such as boron and carbon with an identical electron count as that of Al and Si complexes, respectively, are found to be higher-order saddle points on the PES. This is in accordance with the variable electronic requirements and hence with the instability for the struc-

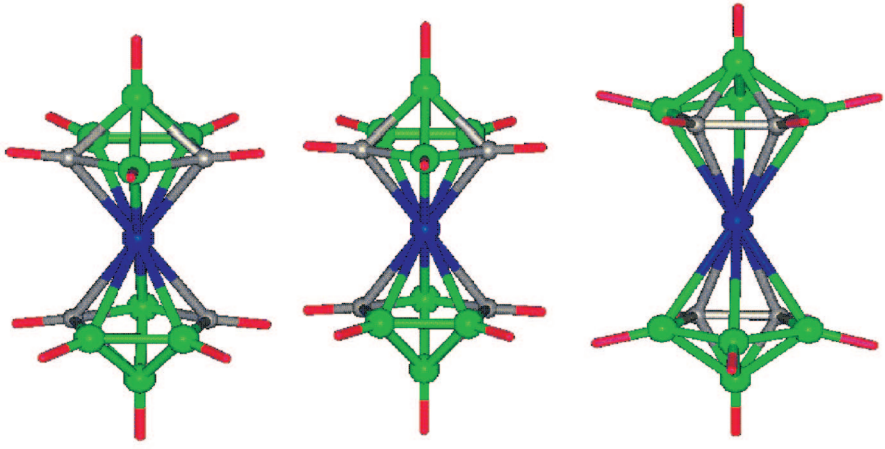

FIG. 6
The optimized geometries of Si, Al, Li single-vertex-sharing systems. The total energies (au) and the low-frequency values (in parentheses) are indicated

tural category of boron bridging complexes in Fig. 3, **D**. The unfavorable interactions of these complexes and the high positive charge of the corresponding endohedral isomers (+5 and +6) preclude them experimentally. The complexes of structural variety **9** are given more attention for several reasons. Icosahedral boranes, carbaboranes, and silaboranes are the more stable members of the polyhedral family and endohedral complexes are most likely to be generated here. Icosahedral $B_{12}H_{12}^{2-}$ is especially favored because of the orbitals of high symmetry with which the central atom can interact perfectly. Trends in the calculational results of the structures and energies are described below.

Energetics and Geometries

The energy involved in the encapsulation (ΔE_{en}) of an atom inside each cage (Fig. 2) is estimated using the equation

$$X^a + Y_mB_nH_{n+m}{}^b \rightarrow X@Y_mB_nH_{n+m}{}^{a+b} , \qquad (1)$$

where X = the central atom, Y = B, C or Si. The central atoms are so chosen as to fit within the cavity of a given polyhedral borane. The central atom should not lead to unduly large negative or positive charge of the complex.

The energy of encapsulation, ΔE_{en} obtained from the equation is tabulated in Table III. The varying charge requirements in the different isomers make it difficult to have a uniform comparison across all the isomers using ΔE_{en}. However, the endohedral carba- and silaboranes can be compared without any ambiguity. While endohedral interactions are ideal in $B_{12}H_{12}^{2-}$, an external perturbation by substituting boron by a heteroatom such as carbon or silicon causes a reduction in symmetry leading to inequivalent interactions of the orbitals of the central atom with the skeletal orbitals. In addition, substitution of a boron atom by a carbon atom reduces slightly the cage size thus making the corresponding endohedral systems more strained. For example, the ΔE_{en} values are 169.8 kcal/mol for $He@B_{12}H_{12}^{2-}$ (**9a-He**), 180.2 kcal/mol for the monocarba-substituted system (**9b-He**) and 191.2 kcal/mol for the dicarbaborane (**9c-He**). The corresponding ΔE_{en} values for the silaboranes are 150.3 and 138.1 kcal/mol, respectively, for **9e-He** and **9f-He** systems. Similar trends continue for Li and Be encapsulation; ΔE_{en} indicates that mono- and disilaboranes with Li and Be as the doped

atom ((**9e-Li**, **9f-Li**); (**9e-Be**, **9f-Be**)) are more stable than the corresponding stuffed carbaboranes ((**9b-Li**, **9c-Li**); (**9b-Be**, **9c-Be**)).

Comparison across different endohedral isomers can be done using the near-isodesmic equations.

$$X@B_nH_n^{a-2} + Y_mB_nH_{n+m}^{b} \rightarrow X@Y_mB_nH_{n+m}^{a+b} + B_nH_n^{2-} \qquad (2)$$

The size of the cage and the size of the central ion play significant role in the energetics of this equation. The He-centered cages have a stability order of **9g-He** > **9f-He** > **9e-He** > **9b-He** > **9c-He** > **9d-He** which is the same as that of the cage size. With Li the stability order changes to **9e-Li** > **9b-Li** > **9f-Li** > **9c-Li** > **9g-Li** > **9d-Li**. This can be attributed to the smaller size of the Li ion and hence is more favorable for monosilaboranes, having maximum positive interaction with the orbitals of central atom and skeleton, rather than disilaboranes where, due to the large size, the bonding interactions are reduced. Li stuffed monocarba- and monosilaboranes being neutral are especially important. Similarly for the Be stuffed systems, the order is **9e-Be** > **9b-Be** > **9f-Be** > **9c-Be** identical to that of the Li-encapsulated systems.

The steric constraints arising from encapsulation is reflected in the geometrical parameters–skeletal bond lengths (Table V) and the estimated percentage of expansion (Table VI). The latter is the percentage change in the distance from the centroid to the atoms on the surface as a result of expansion. The surface B–B distance increases from 1.787 Å in $B_{12}H_{12}^{2-}$ to 1.861 Å in **9a-He**, 1.874 Å in **9a-Li**, 1.871 Å in **9a-Be**, 1.859 Å in **9a-B**, and 1.998 Å in **9a-Ne**. In monocarbaborane-encapsulated systems, the C–B distances are within the range 1.750–1.900 Å. This is higher than the C–B distance (1.707 Å) calculated for the parent cage $CB_{11}H_{12}^{-}$. Similarly the skeletal B–B bond lengths are in the range 1.840-2.050 Å where for the parent system the B–B bond length is well below 1.800 Å. Similar lengthening of skeletal bonds occurs in all the cages.

The percentage of expansion shows that in carbaboranes the largest expansion is observed at the C–H vertices (Table VI). The vertices nearest to the carbon show a larger expansion between the B–H vertices. As one goes to a vertex which is far from the substituted site, the percentage of expansion decreases. In silaboranes this trend is reversed. This shows that the endohedral system adjusts itself to attain a nearly spherical shape so as to enhance the interaction between the orbitals and hence the stability.

TABLE Ia

The total energies[a] (au), zero point vibration energies (ZPVE, kcal/mol), HOMO-LUMO gap (H-L Gap, eV), charge on the central atom (Q(X)) and the lowest frequency (LF) of endohedral complexes $X@C_nB_{12-n}H_{12}^q$ (X = He, Ne, Li, Be; q = charge of the molecule). The relative energies (RE) among the various isomers are given in parentheses wherever necessary

Code	Isomer	Sym-metry	Energy, au (RE, kcal/mol)	ZPVE kcal/mol	H-L Gap eV	Q(X)	LF
9a-He	$He@B_{12}H_{12}^{2-}$	I_h	–308.326599	106.73	8.44	0.10	437.8
9b-He	$He@CB_{11}H_{12}^{-}$	C_1	–321.614225	110.37	8.17	0.10	390.7
9c$_1$-He	$He@p\text{-}C_2B_{10}H_{12}$	D_{5d}	–334.737114(0.0)	113.21	7.92	0.10	354.6
9c$_2$-He	$He@m\text{-}C_2B_{10}H_{12}$	C_{2v}	–334.729926(4.51)	113.30	7.94	0.10	350.7
9c$_3$-He	$He@o\text{-}C_2B_{10}H_{12}$	C_{2v}	–334.71837(15.23)	112.89	7.84	0.10	359.4
9d$_1$-He	$He@1,7,9\text{-}C_3B_9H_{12}^{+}$	C_{3v}	–347.681760(0.0)	115.02	8.00	0.10	324.3
9d$_2$-He	$He@1,2,3\text{-}C_3B_9H_{12}^{+}$	C_{3v}	–347.616409(41.0)	113.74	7.41	0.10	297.6
9d$_3$-He	$He@2,3,4\text{-}C_3B_9H_{12}^{+}$	C_s	–347.637524(27.8)	114.28	7.47	0.10	325.1
9d$_4$-He	$He@2,4,5\text{-}C_3B_9H_{12}^{+}$	C_s	–347.660395(13.4)	114.50	7.77	0.10	318.8
9d$_5$-He	$He@1,2,12\text{-}C_3B_9H_{12}^{+}$	C_s	–347.662260(12.2)	114.54	7.58	0.10	315.2
9a-Li	$Li@B_{12}H_{12}^{-}$	I_h	–313.133455	106.79	8.50	–2.77	414.3
9b-Li	$Li@CB_{11}H_{12}$	C_{5v}	–326.241299	108.97	8.15	–2.54	357.8
9c$_1$-Li	$Li@p\text{-}C_2B_{10}H_{12}^{+}$	D_{5d}	–339.179215(0.0)	110.34	7.82	–2.39	306.1
9c$_2$-Li	$Li@m\text{-}C_2B_{10}H_{12}^{+}$	C_{2v}	–339.178721(0.3)	110.73	7.80	–2.37	319.5
9c$_3$-Li	$Li@o\text{-}C_2B_{10}H_{12}^{+}$	C_s	–339.157362(13.7)	110.43	7.79	–2.38	307.3
9d$_1$-Li	$Li@1,7,9\text{-}C_3B_9H_{12}^{+2}$	C_{3v}	–351.937654(0.0)	110.83	7.79	–2.23	257.1
9d$_2$-Li	$Li@1,2,3\text{-}C_3B_9H_{12}^{+2}$	C_{3v}	–351.874829(39.4)	109.61	7.46	–2.24	211.8
9d$_3$-Li	$Li@2,3,4\text{-}C_3B_9H_{12}^{+2}$	C_s	–351.895419(26.5)	110.15	7.34	–2.24	258.2
9d$_4$-Li	$Li@2,4,5\text{-}C_3B_9H_{12}^{+2}$	C_s	–351.913736(15.01)	110.57	7.60	–2.23	253.5
9d$_5$-Li	$Li@1,2,12C_3B_9H_{12}^{+2}$	C_s	–351.917648(12.6)	110.42	7.66	–2.24	250.8
9a-Be	$Be@B_{12}H_{12}$	I_h	–320.273374	105.66	8.68	1.08	409.7
9b-Be	$Be@CB_{11}H_{12}^{+}$	C_{5v}	–333.200342	106.55	8.26	1.33	340.4
9c$_1$-Be	$Be@p\text{-}C_2B_{10}H_{12}^{+2}$	D_{5d}	–345.948543(1.46)	106.24	7.83	1.42	267.2
9c$_2$-Be	$Be@m\text{-}C_2B_{10}H_{12}^{+2}$	C_{2v}	–345.950874(0.0)	106.50	7.82	1.45	276.7
9c$_3$-Be	$Be@o\text{-}C_2B_{10}H_{12}^{+2}$	C_s	–345.931086(12.41)	106.23	7.82	1.45	279.8
9a-B	$B@B_{12}H_{12}^{+}$	I_h	–329.961162	100.75	7.97	0.37	214.9
9a-Ne	$Ne@B_{12}H_{12}^{2-}$	I_h	–433.948481	97.12	7.51	0.09	290.1
9b-Ne	$Ne@CB_{11}H_{12}^{-}$	C_{5v}	–447.213398	99.57	7.19	0.08	86.8
9a-Ga	$Ga@B_{12}H_{12}^{+}$	I_h	–2 227.892117	104.47	7.68	–4.34	145.3
9a-Si	$Si@B_{12}H_{12}^{+2}$	I_h	–593.993353	95.69	8.05	1.31	219.8
10a-He$_2$	$He_2@B_{17}H_{17}^{2-}$	C_s	–438.409278	153.25	5.86	0.07	129.9
10a-Li$_2$	$Li_2@B_{17}H_{17}$	C_s	–447.717853	150.79	6.22	0.66	87.0
3Al	$[(C_2B_4H_6)_2Al]^{-}$	C_{2h}	–601.094016	110.62	2.11	–0.04	4.1
3Si	$[(C_2B_4H_6)_2Si]$	C_{2h}	–648.009730	111.83	6.25	0.53	27.6
3Li	$[(C_2B_4H_6)_2Li]^{3-}$	C_{2h}	–365.800723	104.61	4.68	–0.53	21.1

[a] The additional total energies required for the equations are $B_{12}H_{12}^{2-}$ –305.69021; $B_{17}H_{17}^{2-}$ –432.99603 (Mebel A. M., Najafian K., Schleyer P. v. R.: *Inorg. Chem.* **1998**, *37*, 6765); $CB_{11}H_{12}^{-}$ –318.994288; $p\text{-}C_2B_{10}H_{12}$ –332.134854; $m\text{-}C_2B_{10}H_{12}$ –332.130514; $o\text{-}C_2B_{10}H_{12}$ –332.104338 (Jemmis E. D., Kiran B.: *J. Am. Chem. Soc.* **1997**, *119*, 4076); $1,7,9\text{-}C_3B_9H_{12}^{+}$ –345.092057; $1,2,3\text{-}C_3B_9H_{12}^{+}$ –345.013573; $2,3,4\text{-}C_3B_9H_{12}^{+}$ –345.039338; $2,4,5\text{-}C_3B_9H_{12}^{+}$ –345.065683; $1,2,12\text{-}C_3B_9H_{12}^{+}$ –345.070426 (Jemmis E. D., Ramalingam M., Jayasree E. G.: *J. Comput. Chem.* **2001**, *22*, 1542).

TABLE Ib

The total energies (au), zero point vibration energies (ZPVE, kcal/mol), the strain energy, the difference between endo and exo isomers (SE), HOMO-LUMO gap (H-L Gap, eV), charge on the central atom (Q(X)) and the lowest frequency (LF) of exo isomers $XC_nB_{12-n}H_{12}^q$ (X = He, Ne, Li, Be; q = charge of the molecule). The relative energies (RE) are given in parentheses wherever necessary

Code	Isomer	Sym-metry	Energy, au (RE, kcal/mol)	ZPVE kcal/mol	SE kcal/mol	H-L Gap eV	Q(X)	LF
9a-He′	$HeB_{12}H_{12}^{2-}$	C_{3v}	–308.597321	104.98	169.88	9.00	0.00	10.4
9b-He′	$HeCB_{11}H_{12}^{-}$	C_s	–321.901584	109.04	180.31	8.79	0.00	20.1
9c$_1$-He′	He*p*-$C_2B_{10}H_{12}$	C_s	–335.041869(0.0)	112.01	191.23	8.59	0.00	–32.4
9c$_2$-He′	He*m*-$C_2B_{10}H_{12}$	C_s	–335.037518(2.7)	111.81	193.01	8.53	0.00	–18.9
9c$_3$-He′	He*o*-$C_2B_{10}H_{12}$	C_s	–335.01165(19.0)	111.48	187.50	8.34	0.00	–17.5
9d$_1$-He′	He1,7,9-$C_3B_9H_{12}^{+}$	C_s	–347.999407(0.0)	113.82	199.32	8.49	0.00	11.9
9d$_2$-He′	He1,2,3-$C_3B_9H_{12}^{+}$	C_s	–347.920910(49.3)	112.63	191.07	7.79	0.00	11.2
9d$_3$-He′	He2,3,4-$C_3B_9H_{12}^{+}$	C_s	–347.946411(33.3)	113.00	193.83	7.93	0.00	–26.7
9d$_4$-He′	He2,4,5-$C_3B_9H_{12}^{+}$	C_s	–347.972982(16.6)	113.47	196.15	8.36	0.00	–7.0
9d$_5$-He′	He1,2,12-$C_3B_9H_{12}^{+}$	C_s	–347.977772(13.6)	113.51	197.98	8.18	0.00	–16.2
9a-Li′	$LiB_{12}H_{12}^{-}$	C_{3v}	–313.318124	107.32	115.88	4.34	0.06	256.7
9b-Li′	$LiCB_{11}H_{12}$	C_s	–326.480831	110.84	150.31	6.02	0.25	210.9
9c$_1$-Li′	Li*p*-$C_2B_{10}H_{12}^{+}$	C_s	–339.464667(3.4)	112.72	179.12	7.37	0.49	140.3
9c$_2$-Li′	Li*m*-$C_2B_{10}H_{12}^{+}$	C_s	–339.470142(0.0)	112.74	182.87	7.68	0.46	139.0
9c$_3$-Li′	Li*o*-$C_2B_{10}H_{12}^{+}$	C_s	–339.440806(18.4)	112.30	177.86	7.36	0.47	129.7
9d$_1$-Li′	Li1,7,9-$C_3B_9H_{12}^{+2}$	C_s	–352.372334(0.0)	113.64	272.76	6.86	1.00	–20.0
9d$_2$-Li′	Li1,2,3-$C_3B_9H_{12}^{+2}$	C_s	–352.225726(92.0)	112.67	220.19	8.01	0.70	59.0
9d$_3$-Li′	Li2,3,4-$C_3B_9H_{12}^{+2}$	C_s	–352.308514(40.1)	112.97	259.22	6.61	1.00	–3.3
9d$_4$-Li′	Li2,4,5-$C_3B_9H_{12}^{+2}$	C_s	–352.333605(24.3)	113.47	263.47	6.70	1.00	6.07
9d$_5$-Li′	Li1,2,12$C_3B_9H_{12}^{+2}$	C_s	–352.340132(20.2)	113.44	265.11	6.76	1.00	–15.0
9a-Be′	$BeB_{12}H_{12}$	C_{3v}	–320.366166	108.45	58.23	3.87	0.05	406.8
9b-Be′	$BeCB_{11}H_{12}^{+}$	C_s	–333.356353	111.38	97.90	4.56	0.22	398.4
9c$_1$-Be′	Be*p*-$C_2B_{10}H_{12}^{+2}$	C_s	–346.140060(11.4)	112.07	120.17	7.11	0.45	362.5
9c$_2$-Be′	Be*m*-$C_2B_{10}H_{12}^{+2}$	C_s	–346.158195(0.0)	112.52	130.10	5.30	0.44	361.8
9c$_3$-Be′	Be*o*-$C_2B_{10}H_{12}^{+2}$	C_s	–346.126925(19.6)	111.98	122.89	4.93	0.42	352.7
9a-B′	$BB_{12}H_{12}^{+}$	C_{3v}	–330.057921	106.21	60.72	3.34	0.40	428.0
9a-Ne′	$NeB_{12}H_{12}^{2-}$	C_{3v}	–434.587324	105.30	400.87	9.00	0.02	47.5
9b-Ne′	$NeCB_{11}H_{12}$	C_s	–447.891856	109.25	425.73	8.79	0.22	51.2
9a-Ga′	$GaB_{12}H_{12}^{+}$	C_{3v}	–2 228.195507	100.50	190.38	2.40	0.55	–207.4
9a-Si′	$SiB_{12}H_{12}^{+2}$	C_{3v}	–594.237695	99.34	153.33	2.76	0.97	–115.4
10a-He$_2$′	$He_2B_{17}H_{17}^{2-}$	C_2	–438.809797	150.13	251.33	7.05	0.00	–17.9
10a-Li$_2$′	$Li_2B_{17}H_{17}$	C_2	–448.086404	154.11	231.27	5.16	0.25	169.8

TABLE IIa

The total energies[a] (au), zero point vibration energies (ZPVE, kcal/mol), HOMO-LUMO gap (H-L Gap, eV), charge on the central atom (Q(X)) and the lowest frequency (LF) of $X@Si_nB_{12-n}H_{12}^q$ (X = He, Li, Be; q = charge of the molecule). The relative energies (RE) are given in parentheses wherever necessary

Code	Isomer	Sym-metry	Energy, au (RE, kcal/mol)	ZPVE kcal/mol	H-L Gap eV	Q(X)	LF
9e-He	$He@SiB_{11}H_{12}^-$	C_{5v}	–573.027881	105.13	7.45	0.10	325.0
9f$_1$-He	$He@p\text{-}Si_2B_{10}H_{12}$	D_{5d}	–837.559458(2.6)	102.68	7.36	0.09	279.2
9f$_2$-He	$He@m\text{-}Si_2B_{10}H_{12}$	C_{2v}	–837.563588(0.0)	102.66	6.31	0.09	177.1
9f$_3$-He	$He@o\text{-}Si_2B_{10}H_{12}$	C_s	–837.563021(0.4)	102.80	6.77	0.09	250.1
9g$_1$-He	$He@1,7,9\text{-}Si_3B_9H_{12}^+$	C_{3v}	–1 101.937307(1.9)	99.42	6.10	0.09	178.4
9g$_2$-He	$He@1,2,3\text{-}Si_3B_9H_{12}^+$	C_{3v}	–1 101.939681(0.4)	99.88	7.53	0.08	241.0
9g$_3$-He	$He@2,3,4\text{-}Si_3B_9H_{12}^+$	C_s	–1 101.940253(0.0)	99.58	7.30	0.08	165.8
9g$_4$-He	$He@2,4,5\text{-}Si_3B_9H_{12}^+$	C_s	–1 101.934355(3.7)	99.61	7.17	0.09	142.7
9g$_5$-He	$He@1,2,12\text{-}Si_3B_9H_{12}^+$	C_s	–1 101.937203(1.9)	99.39	6.62	0.08	168.6
9e-Li	$Li@SiB_{11}H_{12}$	C_{5v}	–577.647834	104.29	6.76	–2.50	309.1
9f$_1$-Li	$Li@p\text{-}Si_2B_{10}H_{12}^+$	D_{5d}	–842.005437(0.0)	100.96	6.53	–2.27	258.0
9f$_2$-Li	$Li@m\text{-}Si_2B_{10}H_{12}^+$	C_{2v}	–842.005406(0.02)	100.86	5.63	–2.26	204.5
9f$_3$-Li	$Li@o\text{-}Si_2B_{10}H_{12}^+$	C_{2v}	–842.002047(2.1)	100.80	6.81	–2.23	229.8
9g$_1$-Li	$Li@1,7,9\text{-}Si_3B_9H_{12}^{+2}$	C_{3v}	–1 106.213376(0.0)	96.68	7.03	–2.06	195.6
9g$_2$-Li	$Li@1,2,3\text{-}Si_3B_9H_{12}^{+2}$	C_{3v}	–1 106.205720(4.8)	96.55	6.71	–2.00	196.9
9g$_3$-Li	$Li@2,3,4\text{-}Si_3B_9H_{12}^{+2}$	C_s	–1 106.206511(4.3)	96.50	5.82	–2.00	147.7
9g$_4$-Li	$Li@2,4,5\text{-}Si_3B_9H_{12}^{+2}$	C_s	–1 106.207960(3.4)	96.81	6.50	–2.04	183.5
9g$_5$-Li	$Li@1,2,12\text{-}Si_3B_9H_{12}^+$	C_s	–1 106.209526(2.4)	96.53	6.66	–2.04	170.7
9e-Be	$Be@SiB_{11}H_{12}^+$	C_{5v}	–584.610558	102.05	7.04	1.31	301.5
9f$_1$-Be	$Be@p\text{-}Si_2B_{10}H_{12}^{+2}$	D_{5d}	–848.794720(1.9)	97.58	6.58	1.29	241.8
9f$_2$-Be	$Be@m\text{-}Si_2B_{10}H_{12}^{+2}$	C_{2v}	–848.797677(0.0)	97.70	6.77	1.32	237.7
9f$_3$-Be	$Be@o\text{-}Si_2B_{10}H_{12}^{+2}$	C_{2v}	–848.792394(3.3)	97.55	6.18	1.17	220.1

[a] The additional total energies required for equations are $SiB_{11}H_{12}^-$ –570.365124; $p\text{-}Si_2B_{10}H_{12}$ –570.365124; $m\text{-}Si_2B_{10}H_{12}$ –834.877723; $o\text{-}Si_2B_{10}H_{12}$ –834.873540 (Jemmis E. D., Kiran B.: *J. Am. Chem. Soc.* **1997**, *119*, 4076); $1,7,9\text{-}Si_3B_9H_{12}^+$ –1 099.232179; $1,2,3\text{-}Si_3B_9H_{12}^+$ –1 099.226018; $2,3,4\text{-}Si_3B_9H_{12}^+$ –1 099.224193 (this study).

TABLE IIb

The energies (au), zero point vibration energies (kcal/mol), HOMO-LUMO gap (H-L Gap, eV), charge on the central atom (Q(X)) and the lowest frequency (LF) of $XSi_nB_{12-n}H_{12}^q$ (X = He, Li, Be; q = charge of the molecule). The relative energies (RE) are given in parentheses wherever necessary

Code	Isomer	Sym-metry	Energy, au (RE, kcal/mol)	ZPVE kcal/mol	SE	H-L Gap eV	Q(X)	LF
9e-He′	$HeSiB_{11}H_{12}^-$	C_s	–573.272118	103.30	153.26	7.77	0.00	–15.0
9f$_1$-He′	He*p*-$Si_2B_{10}H_{12}$	C_s	–837.784746(0.0)	100.74	141.37	7.70	0.00	–22.8
9f$_2$-He′	He*m*-$Si_2B_{10}H_{12}$	C_s	–837.783644(0.69)	100.78	138.09	7.62	0.00	12.0
9f$_3$-He′	He*o*-$Si_2B_{10}H_{12}$	C_s	–837.780544(2.6)	100.73	136.50	6.91	0.00	–32.6
9g$_1$-He′	He1,7,9-$Si_3B_9H_{12}^+$	C_s	–1 102.139225(0.0)	97.52	126.70	7.40	0.00	–17.0
9g$_2$-He′	He1,2,3-$Si_3B_9H_{12}^+$	C_s	–1 102.133134(3.8)	97.55	121.39	6.83	0.00	–8.98
9g$_3$-He′	He2,3,4-$Si_3B_9H_{12}^+$	C_s	–1 102.131276(5.0)	97.52	119.87	6.39	0.00	–16.2
9g$_4$-He′	He2,4,5-$Si_3B_9H_{12}^+$	C_s	–1 102.134649(2.9)	97.69	125.68	6.76	0.00	22.37
9g$_5$-He′	He1,2,12-$Si_3B_9H_{12}^+$	C_s	–1 102.136750(1.6)	97.59	125.22	6.92	0.00	–27.5
9e-Li′	$LiSiB_{11}H_{12}$	C_s	–577.853047	105.16	128.77	6.01	0.25	223.1
9f$_1$-Li′	Li*p*-$Si_2B_{10}H_{12}^+$	C_s	–842.219195(5.5)	101.75	134.13	6.97	0.43	148.4
9f$_2$-Li′	Li*m*-$Si_2B_{10}H_{12}^+$	C_s	–842.227934(0.0)	102.01	139.64	7.21	0.41	170.4
9f$_3$-Li′	Li*o*-$Si_2B_{10}H_{12}^+$	C_s	–842.218991(5.6)	101.86	136.13	6.76	0.44	119.2
9g$_1$-Li′	Li1,7,9-$Si_3B_9H_{12}^{+2}$	C_{3v}	–1 106.450571(3.0)	98.11	148.84	7.42	0.61	101.5
9g$_2$-Li′	Li1,2,3-$Si_3B_9H_{12}^{+2}$	C_s	–1 106.455410(0.0)	98.20	156.68	6.80	0.62	97.0
9g$_3$-Li′	Li2,3,4-$Si_3B_9H_{12}^{+2}$	C_s	–1 106.450856(2.9)	98.13	153.33	6.54	0.66	44.3
9g$_4$-Li′	Li2,4,5-$Si_3B_9H_{12}^{+2}$	C_s	–1 106.449588(3.7)	98.00	151.62	6.84	0.65	–49.1
9g$_5$-Li′	Li1,2,12-$Si_3B_9H_{12}^+$	C_s	–1 106.447016(5.3)	97.83	149.03	6.84	0.64	–10.9
9e-Be′	$BeSiB_{11}H_{12}^+$	C_s	–584.737521	105.85	79.67	4.48	0.20	345.1
9f$_1$-Be′	Be*p*-$Si_2B_{10}H_{12}^{+2}$	C_s	–848.930509(10.9)	102.06	85.21	4.63	0.35	297.8
9f$_2$-Be′	Be*m*-$Si_2B_{10}H_{12}^{+2}$	C_s	–848.947939(0.0)	102.31	94.29	4.85	0.35	264.7
9f$_3$-Be′	Be*o*-$Si_2B_{10}H_{12}^{+2}$	C_s	–848.932801(9.5)	101.97	88.11	4.69	0.34	257.1

Another interesting geometrical feature shown by all the structures is the reduction of the exohedral X–H bonds by the introduction of a central atom. The orbitals of the central atom are found to stabilize some of the bonding molecular orbitals of the cage[14a]. Delocalization of electrons from these exo bonds to the central atom is expected to lengthen the X–H bonds. However, the observed reduction may be attributed to a reduction in the H–X–X–H torsional forces, which would stretch the X–H bonds. A longer X–X distance reduces the torsional strain, leading to a shortening of the X–H bonds. This shortening of X–H bonds is in contrast to endohedral dodecahedrane where lithium insertion shrinks the cage and lengthens the

TABLE IIIa

The energy of encapsulation (kcal/mol) of stuffed systems as obtained from the equation $X^a + Y_mB_nH_{n+m}{}^b \rightarrow X@Y_mB_nH_{n+m}{}^{a+b}$ (X = the central atom, Y = hetero atom on the borane cage, C/Si; a, b, and a+b are the respective charges of the systems)

X	$B_{12}H_{12}^{2-}$	$CB_{11}H_{12}^{-}$	$C_2B_{10}H_{12}$	$C_3B_9H_{12}^{+1}$	$SiB_{11}H_{12}^{-}$	$Si_2B_{10}H_{12}$	$Si_3B_9H_{12}^{+1}$
He	169.8	180.2	191.2	199.1	150.3	138.1	119.9
Ne	399.1	423.7	–	–	–	–	–
Li^+	–99.6	23.6	150.7	275.4	1.2	98.4	190.4
Be^{+2}	–584.2	–347.5	–105.5	–	–372.2	–168.7	–

ΔE_{en} values in addition are $B@B_{12}H_{12}^{+}$ –1 413.6, $Ga@B_{12}H_{12}^{+}$ –898.7, $Si@B_{12}H_{12}^{+2}$ –1 723.6.

TABLE IIIb

The energy of capping (kcal/mol) of systems as obtained from the equationn $X^a + Y_mB_nH_{n+m}{}^b \rightarrow XY_mB_nH_{n+m}{}^{a+b}$ (X = the capping atom, Y = hetero atom on the borane cage, C/Si; a, b, and a+b are the respective charges of the systems)

X	$B_{12}H_{12}^{2-}$	$CB_{11}H_{12}^{-}$	$C_2B_{10}H_{12}$	$C_3B_9H_{12}^{+1}$	$SiB_{11}H_{12}^{-}$	$Si_2B_{10}H_{12}$	$Si_3B_9H_{12}^{+1}$
He	–0.04	–0.2	0.02	–0.19	0.03	0.02	0.002
Ne	–1.7	–2.0	–	–	–	–	–
Li^+	–215.5	–126.8	–34.6	2.7	–127.6	–41.9	34.6
Be^{+2}	–642.4	–445.4	–235.6	–	–451.9	–263.0	–

ΔE_{en} values in addition are $B_{13}H_{12}^{+}$ –1 474.3, $GaB_{12}H_{12}^{+}$ –1 089.0, $SiB_{12}H_{12}^{+2}$ –1 876.9.

TABLE IV

The ΔE values obtained from the near isodesmic equations of the form $X@B_nH_n^{a-2} + Y_mB_nH_{n+m}^{b} \rightarrow X@Y_mB_nH_{n+m}^{a+b} + B_nH_n^{2-}$ (X = the central atom, Y = hetero atom on the borane cage, C/Si; a–2, a+b, and b are the respective charges of the system)

LHS		RHS		ΔE, kcal/mol
$He@B_{12}H_{12}^{2-}$	$CB_{11}H_{12}^{-}$	$He@CB_{11}H_{12}^{-}$	$B_{12}H_{12}^{2-}$	10.32
$He@B_{12}H_{12}^{2-}$	*p*-$C_2B_{10}H_{12}$	He@*p*-$C_2B_{10}H_{12}$	$B_{12}H_{12}^{2-}$	21.42
$He@B_{12}H_{12}^{2-}$	1,7,9-$C_3B_9H_{12}^{+}$	He@1,7,9-$C_3B_9H_{12}^{+}$	$B_{12}H_{12}^{2-}$	29.30
$He@B_{12}H_{12}^{2-} > He@CB_{11}H_{12}^{-} > He@$*p*-$C_2B_{10}H_{12} > He@$1,7,9-$C_3B_9H_{12}^{+}$				
$Li@B_{12}H_{12}^{-}$	$CB_{11}H_{12}^{-}$	$Li@CB_{11}H_{12}$	$B_{12}H_{12}^{2-}$	123.14
$Li@B_{12}H_{12}^{-}$	*p*-$C_2B_{10}H_{12}$	Li@*p*-$C_2B_{10}H_{12}^{+}$	$B_{12}H_{12}^{2-}$	250.30
$Li@B_{12}H_{12}^{-}$	1,7,9-$C_3B_9H_{12}^{+}$	Li@1,7,9-$C_3B_9H_{12}^{+2}$	$B_{12}H_{12}^{2-}$	375.02
$Li@B_{12}H_{12}^{-} > Li@CB_{11}H_{12} > Li@$*p*-$C_2B_{10}H_{12}^{+} > Li@$1,7,9-$C_3B_9H_{12}^{+2}$				
$Be@B_{12}H_{12}$	$CB_{11}H_{12}^{-}$	$Be@CB_{11}H_{12}^{+}$	$B_{12}H_{12}^{2-}$	236.64
$Be@B_{12}H_{12}$	*m*-$C_2B_{10}H_{12}$	Be@*m*-$C_2B_{10}H_{12}^{+2}$	$B_{12}H_{12}^{2-}$	478.66
$Be@B_{12}H_{12} > Be@CB_{11}H_{12}^{+} > Be@$*m*-$C_2B_{10}H_{12}^{+2}$				
$Ne@B_{12}H_{12}^{2-}$	$CB_{11}H_{12}^{-}$	$Ne@CB_{11}H_{12}^{-}$	$B_{12}H_{12}^{2-}$	24.58
$Ne@B_{12}H_{12}^{2-} > Ne@CB_{11}H_{12}^{-}$				
$He@B_{12}H_{12}^{2-}$	$SiB_{11}H_{12}^{-}$	$He@SiB_{11}H_{12}^{-}$	$B_{12}H_{12}^{2-}$	–16.54
$He@B_{12}H_{12}^{2-}$	*m*-$Si_2B_{10}H_{12}$	He@*m*-$Si_2B_{10}H_{12}$	$B_{12}H_{12}^{2-}$	–31.78
$He@B_{12}H_{12}^{2-}$	2,3,4-$Si_3B_9H_{12}^{+}$	He@2,3,4-$Si_3B_9H_{12}^{+}$	$B_{12}H_{12}^{2-}$	–50.00
$He@$2,3,4-$Si_3B_9H_{12}^{+} > He@$*m*-$Si_2B_{10}H_{12} > He@SiB_{11}H_{12}^{-} > He@B_{12}H_{12}^{2-}$				
$Li@B_{12}H_{12}^{-}$	$SiB_{11}H_{12}^{-}$	$Li@SiB_{11}H_{12}$	$B_{12}H_{12}^{2-}$	100.74
$Li@B_{12}H_{12}^{-}$	*p*-$Si_2B_{10}H_{12}$	Li@*p*-$Si_2B_{10}H_{12}^{+}$	$B_{12}H_{12}^{2-}$	197.99
$Li@B_{12}H_{12}^{-}$	1,7,9-$Si_3B_9H_{12}^{+}$	Li@1,7,9-$Si_3B_9H_{12}^{+2}$	$B_{12}H_{12}^{2-}$	289.94
$Li@B_{12}H_{12}^{-} > Li@$*p*-$Si_2B_{10}H_{12}^{+} > Li@SiB_{11}H_{12} > Li@$1,7,9-$Si_3B_9H_{12}^{+2}$				
$Be@B_{12}H_{12}$	$SiB_{11}H_{12}^{-}$	$Be@SiB_{11}H_{12}^{+}$	$B_{12}H_{12}^{2-}$	211.93
$Be@B_{12}H_{12}$	*m*-$Si_2B_{10}H_{12}$	Be@*m*-$Si_2B_{10}H_{12}^{+2}$	$B_{12}H_{12}^{2-}$	415.43
$Be@B_{12}H_{12} > Be@$*m*-$Si_2B_{10}H_{12}^{+2} > Be@SiB_{11}H_{12}^{+}$				

TABLE Va
Skeletal bond lengths of $X@C_mB_nH_{n+m}^{a+b}$ calculated at B3LYP/6-31G*

Doped atom	Skeletal bond lengths (Å) of endohedral $CB_{11}H_{12}^-$ systems				
	$C–B_a$	$B_a–B_a$	$B_a–B_b$	$B_b–B_b$	$B_b–B_c$
He	1.779	1.843	1.850	1.869	1.876
Li	1.796	1.866	1.863	1.888	1.897
Be	1.792	1.871	1.860	1.898	1.916
Ne	1.885	1.952	1.969	2.054	2.089

	Skeletal bond lengths (Å) of endohedral *p*-$C_2B_{10}H_{12}$ systems		
	$C–B_a/C–B_b$	$B_a–B_b$	$B_a–B_a/B_b–B_b$
He	1.794	1.845	1.852
Li	1.818	1.860	1.884
Be	1.830	1.859	1.904

	Skeletal bond lengths (Å) of endohedral *m*-$C_2B_{10}H_{12}$ systems									
	$C–B_a$	$C–B_b$	$C–B_c$	$B_a–B_a$	$B_b–B_b$	$B_d–B_d$	$B_a–B_b$	$B_b–B_c$	$B_b–B_d$	$B_c–B_d$
He	1.792	1.783	1.774	1.847	1.841	1.879	1.831	1.861	1.863	1.862
Li	1.774	1.815	1.837	1.881	1.859	1.905	1.851	1.893	1.887	1.892
Be	1.767	1.818	1.863	1.896	1.854	1.951	1.857	1.925	1.902	1.910

	Skeletal bond lengths (Å) of endohedral *o*-$C_2B_{10}H_{12}$ systems									
	$C–B_a$	$C–B_b$	C–C	$B_b–B_b$	$B_d–B_d$	$B_a–B_b$	$B_a–B_c$	$B_b–B_c$	$B_b–B_d$	$B_c–B_d$
He	1.778	1.778	1.698	1.852	1.884	1.846	1.842	1.862	1.869	1.888
Li	1.801	1.794	1.709	1.880	1.921	1.870	1.850	1.881	1.890	1.923
Be	1.811	1.787	1.695	1.895	1.974	1.872	1.848	1.889	1.912	1.961

TABLE Vb
Skeletal bond lengths of $X@Si_mB_nH_{n+m}^{a+b}$ calculated at B3LYP/6-31G*

Doped atom	Skeletal bond lengths (Å) of endohedral $SiB_{11}H_{12}^-$ systems				
	Si–B_a	B_a–B_a	B_a–B_b	B_b–B_b	B_b–B_c
He	2.126	1.996	1.831	1.862	1.837
Li	2.139	1.976	1.852	1.880	1.863
Be	2.130	1.942	1.858	1.889	1.877

	Skeletal bond lengths (Å) of endohedral *p*-$Si_2B_{10}H_{12}$ systems		
	Si–B_a/Si–B_b	B_a–B_b	B_a–B_a/B_b–B_b
He	1.991	1.811	1.994
Li	2.138	1.831	1.985
Be	2.149	1.837	1.965

	Skeletal bond lengths (Å) of endohedral *m*-$Si_2B_{10}H_{12}$ systems									
	Si–B_a	Si–B_b	Si–B_c	B_a–B_a	B_b–B_b	B_d–B_d	B_a–B_b	B_b–B_c	B_b–B_d	B_c–B_d
He	2.143	2.145	2.107	2.510	1.816	1.836	1.875	1.941	1.836	1.821
Li	2.137	2.160	2.130	2.217	1.827	1.880	1.913	1.957	1.861	1.849
Be	2.135	2.156	2.137	2.031	1.844	1.912	1.914	1.945	1.878	1.865

	Skeletal bond lengths (Å) of endohedral *o*-$Si_2B_{10}H_{12}$ systems									
	Si–B_a	Si–B_b	Si–Si	B_b–B_b	B_d–B_d	B_a–B_b	B_a–B_c	B_b–B_c	B_b–B_d	B_c–B_d
He	2.281	2.103	2.395	2.010	1.821	1.936	1.798	1.831	1.819	1.834
Li	2.268	2.122	2.437	2.001	1.850	1.941	1.833	1.854	1.848	1.865
Be	2.225	2.124	2.443	1.974	1.878	1.922	1.864	1.865	1.867	1.893

TABLE VIa
Distance from the central atom (X) to each of the vertices in $X@C_mB_nH_{n+m}^{a+b}$. Corresponding percentage of expansion is given in parentheses

Doped atom	Distance from X to the surface atoms (Å) in stuffed $CB_{11}H_{12}^-$			
	C	B_a	B_b	B_c
He	1.681(8.3)	1.778(4.8)	1.750(3.3)	1.729(3.2)
Li	1.692(9.0)	1.801(6.1)	1.764(3.9)	1.740(4.1)
Be	1.725(11.2)	1.830(7.4)	1.748(4.5)	1.704(0.6)
Ne	1.860(19.8)	1.923(13.3)	1.880(12.3)	1.838(8.8)

	Distance from X to the surface atoms (Å) in stuffed *p*-$C_2B_{10}H_{12}$	
	C	B_a/B_b
He	1.641(7.5)	1.760(3.8)
Li	1.646(7.8)	1.785(5.3)
Be	1.636(7.1)	1.799(6.2)

	Distance from X to the surface atoms (Å) in stuffed *m*-$C_2B_{10}H_{12}$				
	C	B_a	B_b	B_c	B_d
He	1.660(7.2)	1.793(5.7)	1.762(3.8)	1.734(3.3)	1.733(2.7)
Li	1.678(8.4)	1.833(8.0)	1.787(5.3)	1.755(4.7)	1.741(3.2)
Be	1.700(9.8)	1.908(12.5)	1.803(6.3)	1.744(4.0)	1.709(1.3)

	Distance from X to the surface atoms (Å) in stuffed *o*-$C_2B_{10}H_{12}$				
	C	B_a	B_b	B_c	B_d
He	1.687(8.6)	1.798(4.9)	1.765(4.1)	1.740(3.0)	1.719(2.9)
Li	1.717(10.5)	1.840(7.4)	1.790(5.5)	1.748(3.4)	1.721(3.0)
Be	1.780(14.5)	1.906(11.2)	1.804(6.5)	1.727(2.2)	1.684(0.8)

TABLE VIb
Distance from the central atom (X) to each of the vertices in $X@Si_mB_nH_{n+m}^{a+b}$. Corresponding percentage of expansion is given in parentheses

Doped atom	Distance from X to the surface atoms (Å) in stuffed $SiB_{11}H_{12}^-$			
	Si	B_a	B_b	B_c
He	1.877(–4.6)	1.801(2.5)	1.833(8.1)	1.854(8.5)
Li	2.023(3.1)	1.823(3.8)	1.808(6.7)	1.800(5.3)
Be	2.128(8.2)	1.824(4.0)	1.786(5.4)	1.749(2.3)

	Distance from X to the surface atoms (Å) in stuffed *p*-$Si_2B_{10}H_{12}$	
	Si	B_a/B_b
He	1.991(0.5)	1.850(4.8)
Li	2.063(4.1)	1.849(4.8)
Be	2.110(6.5)	1.836(4.0)

	Distance from X to the surface atoms (Å) in stuffed *m*-$Si_2B_{10}H_{12}$				
	Si	B_a	B_b	B_c	B_d
He	1.933(–0.1)	1.854(2.5)	1.865(5.7)	1.879(7.6)	1.909(10.9)
Li	2.065(3.5)	1.868(3.3)	1.850(4.9)	1.835(5.1)	1.839(6.9)
Be	2.150(7.8)	1.862(3.0)	1.833(3.9)	1.797(2.9)	1.802(4.7)

	Distance from X to the surface atoms (Å) in stuffed *o*-$Si_2B_{10}H_{12}$				
	Si	B_a	B_b	B_c	B_d
He	1.919(–6.0)	1.832(1.2)	1.865(6.1)	1.907(10.7)	1.925(12.6)
Li	2.076(1.7)	1.865(3.0)	1.849(5.2)	1.846(7.2)	1.836(7.4)
Be	2.202(7.8)	1.881(3.9)	1.825(3.9)	1.800(4.5)	1.763(3.2)

exo bonds[23]. This contrasting behavior results from the saturated nature of the $C_{20}H_{20}$ skeleton, the extra electron brought by encapsulation of Li occupies molecular orbital which is the bonding combination of the C–H σ* orbitals. In polyhedral boranes, the process of encapsulation enlarges the cage thus increasing the B–B bonds, which in turn decreases the H–B–B–H torsion forces. This results in the shortening of the B–H bonds.

The polarization observed on the central atom is given in Tables I and II. In general the noble gases He and Ne do not show any significant charge transfer. Be and Li show rather high polarization. The abnormal charges on the Li atom obtained for Mulliken population analysis in the endohedral complexes prompted us to look at the natural charges. In all the endohedral systems lithium shows a natural charge of 0.6. The central atom in higher carbon substituted borane shows a greater positive charge. This can be attributed to the enhanced electron withdrawing character of the cage as the number of carbon substitution increases[24]. This trend is also observed in the silaborane-stuffed cages. In endohedral carbaboranes the HOMO-LUMO gap decreases in the range 0.2–0.5 eV as the number of carbon increases even though there is a significant gap.

The multiatom encapsulation in polyhedral boranes has not been considered before. We predict here two examples of two atom-doped *closo* polyhedra (**10**). $He_2@B_{17}H_{17}^{2-}$ (**10a-He$_2$**) and $Li_2@B_{17}H_{17}$ (**10a-Li$_2$**) are found to be minima on the potential energy surfaces with lowest frequencies 87.0 and 129.9. The B–B skeletal distances in both the systems exhibit higher values than the parent $B_{17}H_{17}^{2-}$. The ΔE_{en} value for $He_2@B_{17}H_{17}^{2-}$ is 251.53 kcal/mol and that of $Li_2@B_{17}H_{17}$ is –95.84 kcal/mol. The exothermic value of $Li_2@B_{17}H_{17}$ is comparable to the ΔE_{en} value of $Li@B_{12}H_{12}^{-}$. As shown in Fig. 5, He_2-encapsulated complex requires 2 more electrons and its lithium counterpart is neutral. Even though the lithium atoms are surprisingly close (1.431 Å) no bonding is observed between them. The Li–Li Wiberg bond index (WBI) from the NBO [25] analysis is only 0.036. It shows that the two Li atoms exist as cations, which are very small in size, within the cage and are stabilized by the surrounding anionic cage.

Comparison of the Stability of Endohedral Complexes with Exohedral Face Capped Systems

All the exohedral isomers are more favorable than the endohedral isomers. The relative energies calculated for the stuffed systems with respect to the face capped isomers give a rough estimate of the strain energy involved in encapsulation of a heteroatom (SE, shown in Tables Ib and IIb). These iso-

mers obey the capping principle[26] as well as the *mno* rule[17]. Among the carbaboranes the least strain energy has been evaluated for Be-doped systems. $Be@CB_{11}H_{12}^{+}$ (**9b-Be**) has a strain energy of 97.9 kcal/mol. Similarly the $Be@C_2B_{10}H_{12}^{+2}$ (**9c-Be**) isomers have a strain energy of 120–130 kcal/mol. $Li@CB_{11}H_{12}$ (**9b-Li**) has the value of 150.3 kcal/mol whereas $Li@C_2B_{10}H_{12}^{+}$ (**9c-Li**) isomers show the strain within a range of 175–179 kcal/mol. The comparatively bigger Ne atom has the highest strain with its encapsulated isomer (**9a-Ne**) less stable by 425.73 kcal/mol compared to the corresponding capped isomer (**9a-Ne′**). All the He-face-capped isomers have very low values for the lowest frequency with some of them exhibiting an imaginary value even though they are lower in energy than the endohedral isomers. The isomer in which both the lithium atoms are capped on the trigonal faces of the $B_{17}H_{17}^{2-}$ (**9a-Li$_2$′**) gives a strain energy of 231.27 kcal/mol for the endohedral structure. Silaboranes with their large size show a low value for the strain energy when compared to the endohedral carbaboranes.

The experimental realization of endohedral dodecahedrane is achieved by following the methodology of synthesis of endohedral fullerenes by exposing the cluster to a beam of the encapsulating atom or ion[13e]. The encapsulated boranes could be obtained using the successful experimental routes to related main-group clusters. Several interstitial transition metal clusters are known which can be related to polyhedral boranes through isolobal analogy[27]. Stone has shown that it is possible to have a similar synthetic procedure for isolobally related systems[28]. Another possible way to get the stuffed system is the reduction of the corresponding sandwich structures.

CONCLUSION

The electronic structure of the unexplored endohedral cluster is well explained by fragment molecular orbital treatment by correlating with the experimentally known sandwich structures. Though sandwich complexes are identical to stuffed boranes in molecular composition, the molecular orbital approach shows how they form a separate class of compounds due to their disparate electronic requirements. A comparison with the corresponding exo isomer and their specific geometrical features enable to decide on the stability of the given endohedral cluster. The stability depends on the cage size and the size of the central atom or ion. With the same central atom, the cage size becomes the predominant factor in deciding the stability of the endohedral structures. The geometries and relative energies point out that more symmetrical icosahedral $B_{12}H_{12}^{2-}$ is the most favorable system

for encapsulating an atom inside. The endohedral carbaborane systems are relatively less favorable due to the small cage size than the corresponding endohedral silaborane systems. Qualitative analysis explains the electron counts observed for the polyhedral structures with single-atom bridging and the corresponding endohedral complexes.

The authors thank the Council of Scientific and Industrial Research (CSIR) and Board of Research in Nuclear Science (BRNS) for providing financial support for this work. E. G. Jayasree gratefully acknowledges a Senior Research Fellowship from CSIR. We thank Dr M. M. Balakrishnarajan for his initial contribution to this project.

REFERENCES

1. a) Togni A., Halterman R. L. (Eds): *Metallocenes: Synthesis, Reactivity, Applications*. Wiley-VCH, Weinheim 1998; b) Long N. J.: *Metallocenes*. Blackwell Science, Oxford (U.K.) 1998.
2. a) Siriwardane U., Islam M. S., West T. A., Hosmane N. S., Maguire J. A., Cowley A. H.: *J. Am. Chem. Soc.* **1987**, 109, 4600; b) Hosmane N. S., de Meester P., Siriwardane U., Islam M. S., Chu S. S. C.: *J. Chem. Soc., Chem. Commun.* **1986**, 1421.
3. Hosmane N. S., Lu K. J., Zhang H., Maguire J. A.: *Organometallics* **1997**, *16*, 5163.
4. a) Hosmane N. S., de Meester P., Siriwardane U., Islam M. S., Chu S. S. C.: *J. Am. Chem. Soc.* **1986**, *108*, 6050; b) Islam M. S., Siriwardane U., Hosmane N. S., Maguire J. A., de Meester P., Chu S. S. C.: *Organometallics* **1987**, *6*, 1936.
5. Hosmane N. S., Zhu D., McDonald J. E., Zhang H., Maguire J. A., Gray T. G., Helfert S. C.: *J. Am. Chem. Soc.* **1995**, *117*, 12362.
6. Hosmane N. S., Yang J., Zhang H., Maguire J. A.: *J. Am. Chem. Soc.* **1996**, *118*, 5150.
7. Grimes R. N.: *Metal Interactions with Boron Clusters*. Plenum Press, New York 1982.
8. a) Schubert D. M., Rees W. S., Jr., Knobler C. B., Hawthorne M. F.: *Organometallics* **1990**, *9*, 2938; b) Rees, W. S., Jr., Schubert D. M., Knobler C. B., Hawthorne M. F.: *J. Am. Chem. Soc.* **1986**, *108*, 5369.
9. a) Bandman M. A., Knobler C. B., Hawthorne M. F.: *Inorg. Chem.* **1988**, *27*, 2399; b) Bandman M. A., Knobler C. B., Hawthorne M. F.: *Inorg. Chem.* **1989**, *28*, 1204; c) Schubert D. M., Bandman M. A., Rees W. S., Jr., Knobler C. B., Lu P., Nam W., Hawthorne M. F.: *Organometallics* **1990**, *9*, 2046; d) Rees W. S., Jr., Schubert D. M., Knobler C. B., Hawthorne M. F.: *J. Am. Chem. Soc.* **1986**, *108*, 5367.
10. a) Borodinsky L., Sinn E., Grimes R. N.: *Inorg. Chem.* **1982**, *21*, 1686; b) Xie Z., Jelinek T., Bau R., Reed C. A.: *J. Am. Chem. Soc.* **1994**, *116*, 1907; c) Churchill M. R., Gold K.: *J. Am. Chem. Soc.* **1970**, *92*, 1180; d) Kang H. C., Lee S. S., Knobler C. B., Hawthorne M. F.: *Inorg. Chem.* **1991**, *30*, 2024; e) St. Clair D., Zalkin A., Templeton D. H.: *J. Am. Chem. Soc.* **1970**, *92*, 1173; f) Viñas C., Pedrajas J., Bertran J., Teixidor F., Kivekas R., Sillanpaa R.: *Inorg. Chem.* **1997**, *36*, 2482; g) Hansen F. V., Hazell R. G., Hyatt C., Stucky G. D.: *Acta Chem. Scand.* **1973**, *27*, 1210; i) Yan Y., Mingos D. M. P., Williams D. J., Kurmoo M.: *J. Chem. Soc., Dalton Trans.* **1995**, 3221; j) Plešek J., Heřmánek S., Franken A., Císařová I., Nachtigal C.: *Collect. Czech. Chem. Commun.* **1997**, *62*, 47; k) Plešek J., Štíbr B., Cooke P. A., Kennedy J. D., McGrath T. D., Thornton-Pett M.: *Acta*

Crystallogr., Sect. C: Cryst. Struct. Commun. **1998**, *54*, 36; l) Franken A., Plešek J., Fusek J., Semrau M.: *Collect. Czech. Chem. Commun.* **1997**, *62*, 1070; m) Yan Y., Mingos D. M. P., Muller T. E., Williams D. J., Kurmoo M.: *J. Chem. Soc., Dalton Trans.* **1994**, 1735.

11. Kester J. G., Keller D., Huffman J. C., Benefiel M. A., Geiger W. E., Jr., Atwood C., Siedle A. R., Korba G. A., Todd L. J.: *Inorg. Chem.* **1994**, *33*, 5438.
12. a) Hawthorne M. F., Young D. C., Wegner P. A.: *J. Am. Chem. Soc.* **1965**, *87*, 1818; b) Hawthorne M. F.: *Acc. Chem. Res.* **1968**, *1*, 281; c) Grimes R. N.: *J. Organomet. Chem.* **1999**, *581*, 1; d) Fehlner T. P.: *Struct. Bonding (Berlin)* **1997**, *87*, 112; e) Fehlner T. P.: *Organometallics* **2000**, *19*, 2643.
13. a) Hirsch A., Chen Z., Jiao H.: *Angew. Chem., Int. Ed.* **2000**, *39*, 3915; b) Bühl M.: *Chem. Eur. J.* **1998**, *4*, 734; c) Rubin Y., Jarrosson T., Wang G.-W., Bartberger M. D., Houk K. N., Schick G., Saunders M., Cross R. J.: *Angew. Chem., Int. Ed.* **2001**, *40*, 1543; d) Shabtai E., Weitz A., Haddon R. C., Hoffman R. E., Rabinovitz M., Khong A., Cross R. J., Saunders M., Cheng P.-C., Scott L. T.: *J. Am. Chem. Soc.* **1998**, *120*, 6389; e) Cross R. J., Saunders M., Prinzbach H.: *Org. Lett.* **1999**, *1*, 1479.
14. a) Jemmis E. D., Balakrishnarajan M. M.: *J. Am. Chem. Soc.* **2000**, *122*, 7392; b) Charkin O. P., Klimenko N. M., Moran D., Mebel A. M., Schleyer P. v. R.: *Russ. J. Inorg. Chem.* **2001**, *46*, 110; c) Charkin O. P., Klimenko N. M., Schleyer P. v. R.: *Russ. J. Inorg. Chem.* **2000**, *45*, 1539; d) Charkin O. P., Klimenko N. M., Moran D., Mebel A. M., Charkin D. O., Schleyer P. v. R.: *Inorg. Chem.* **2001**, *40*, 6913.
15. a) Hughes R. E., Kennard C. H. L., Sullinger K. G., Weakliem H. A., Sands D. E., Hoard J. L.: *J. Am. Chem. Soc.* **1963**, *85*, 361; b) Hoard J. L., Sullinger D. B., Kennard C. H. L., Hughes R. E.: *J. Solid State Chem.* **1970**, *1*, 268; c) Jemmis E. D., Balakrishnarajan M. M.: *J. Am. Chem. Soc.* **2001**, *123*, 4324.
16. Srinivas G. N., Hamilton T. P., Jemmis E. D., McKee M. L., Lammertsma K.: *J. Am. Chem. Soc.* **2000**, *122*, 1725.
17. a) Wade K.: *Chem. Commun.* **1971**, 792; b) Wade K.: *Adv. Inorg. Chem. Radiochem.* **1976**, *18*, 1; c) Jemmis E. D., Balakrishnarajan M. M., Pancharatna P. D.: *J. Am. Chem. Soc.* **2001**, *123*, 4313; d) Balakrishnarajan M. M., Jemmis E. D.: *J. Am. Chem. Soc.* **2000**, *122*, 4516; e) Jemmis E. D., Balakrishnarajan M. M., Pancharatna P. D.: *Chem. Rev. (Washington, D. C.)* **2002**, *102*, 93.
18. a) Hoffmann R., Lipscomb W. N.: *J. Chem. Phys.* **1962**, *36*, 2179; b) Hoffmann R.: *J. Chem. Phys.* **1963**, *39*, 1397.
19. a) Becke A. D.: *J. Chem. Phys.* **1993**, *98*, 5648; b) Lee C., Yang W., Parr R. G.: *Phys. Rev. B: Condens. Mater.* **1988**, *37*, 785; c) Vosko S. H., Wilk L., Nusair M.: *Can. J. Phys.* **1980**, *58*, 1200; d) Stephens P. J., Delvin F. J., Chabalowski C. F., Frisch M. J.: *J. Phys. Chem.* **1994**, *98*, 11623.
20. Frisch M. J., Trucks G. W., Schelegel H. B., Gill P. M. W., Johnson B. G., Robb M. A., Cheeseman J. R., Keith T., Peterson G. A., Montgomery J. A., Raghavachari K., Al-Laham M. A., Zakrzewski V. G., Ortiz J. V., Foresman J. B., Cioslowsky J., Stefenov B. B., Nanayakkara A., Challacombe M., Peng C. Y., Ayala P. Y., Chen W., Wong M. W., Andres J. L., Replogle E. S., Gomberts R., Martin R. L., Fox D. J., Binkley J. S., Defrees D. J., Baker J., Stewart J. P., Head-Gordon M., Gonzalez C., Pople J. A.: *Gaussian94, Revision D.1*. Gaussian Inc., Pittsburg (PA) 1995.
21. Pipal J. R., Maxwell W. M., Grimes R. N.: *Inorg. Chem.* **1978**, *17*, 1447.
22. a) Brain P. T., Bühl M., Cowie J., Lewis Z. G., Welch A. J.: *J. Chem. Soc., Dalton. Trans.* **1996**, 231; b) Rosair G. M., Welch A. J., Weller A. S.: *Organometallics* **1998**, *17*, 3227;

c) McWhannell M. A., Rosair G. M., Welch A. J., Teixidor F., Viñas C.: *J. Organomet. Chem.* **1999**, *573*, 165.
23. Moran D., Stahl F., Jemmis E. D., Schaefer H. F., III, Schleyer P. v. R.: *J. Phys. Chem.* **2002**, *106*, 5144.
24. Hawthorne M. F., Benry T. E., Wegner P. A.: *J. Am. Chem. Soc.* **1965**, *87*, 4746; b) Leites L. A., Vinagradova L. E., Kalinin V. N., Zakharkin L. I.: *Izv. Akad. Nauk SSSR, Ser. Khim.* **1970**, 2596.
25. a) Reed A. E., Weistock R. B., Weinhold F.: *J. Chem. Phys.* **1985**, *83*, 735; b) Reed A. E., Curtiss L. A., Weinhold F.: *Chem. Rev. (Washington, D. C.)* **1988**, *88*, 899; c) Wiberg K. B.: *Tetrahedron* **1968**, *24*, 1083.
26. Mingos D. M. P.: *Nat. Phys. Sci.* **1972**, *236*, 99.
27. Hoffmann R.: *Angew. Chem., Int. Ed. Engl.* **1982**, *21*, 711.
28. Stone F. G. A.: *Angew. Chem., Int. Ed. Engl.* **1984**, *23*, 89.